Düzce University Journal of Science & Technology

Research Article

The Influence of Particle Size and Reinforcement Rate of B_4C on Mechanical and Microstructure Properties of Al-B_4C Composites

Mahmut Can ŞENEL*, Mevlüt GÜRBÜZ

Mechanical Engineering Department, Faculty of Engineering, Ondokuz Mayıs University, Samsun, TURKEY
** Corresponding author: mahmutcan.senel@omu.edu.tr*
DOİ: 10.29130/dubited.683876

ABSTRACT

In this study, Al-B_4C composites were produced with various particle sizes (B_4C: 3.5 and 20 µm) and reinforcement rates (B_4C%: 1, 3, 6, 9, 12, 15, 30%) by the powder metallurgy method. The apparent density, compressive strength, and Vickers hardness of the composites were determined by Archimedes' density meter, universal test machine, and micro Vickers hardness measurement device, respectively. The phase and microstructural analysis of the fabricated composites were analyzed using an X-ray diffraction device and scanning electron microscope, respectively. From the test results, the highest micro Vickers hardness (68.8 HV), apparent density (2.61 g/cm^3), compressive strength (242 MPa), and minimum porosity (1.4%) were determined at 3.5 µm particle size and 30% reinforcement rate of B_4C. The enhancement in Vickers hardness and compressive strength of Al-30%B_4C composite was detected as +129.3% and +165.9% compared with pure aluminum.

Keywords: *Aluminum, Boron Carbide, Composite, Hardness, Microstructure*

Partikül Boyutunun ve B_4C Katkı Oranının Al-B_4C Kompozitlerin Mekanik ve Mikroyapı Özellikleri Üzerine Olan Etkisi

ÖZET

Bu çalışmada, Al-B_4C kompozitler farklı partikül boyutlarında (B_4C: 3.5 ve 20 um) ve takviye oranlarında (% B_4C: 1, 3, 6, 9, 12, 15, 30) toz metalürjisi yöntemiyle üretilmiştir. Kompozitlerin görünür yoğunluğu, basma dayanımı ve Vickers sertliği sırasıyla; Arşimet yoğunluk ölçüm cihazı, üniversal test makinesi ve mikro Vickers sertlik ölçüm cihazıyla belirlenmiştir. Üretilen kompozitlerin faz ve mikro-yapı analizi sırasıyla; X-ışını kırınımı cihazı ve taramalı elektron mikroskobu kullanılarak analiz edilmiştir. Test sonuçlarına göre; en yüksek mikro Vickers sertliği (68.8 HV), görünür yoğunluk (2.61 g/cm^3), basma dayanımı (242 MPa) ve en düşük gözeneklilik oranı (% 1.4) %30 B_4C katkı oranına ve 3.5 µm B_4C partikül boyutuna sahip Al-B_4C kompozit yapıda elde edilmiştir. Saf alüminyum ile karşılaştırıldığında Al-%30B_4C kompozitin Vickers sertliğinin ve basma dayanımının sırasıyla; %129.3 ve %165.9 oranında arttığı tespit edilmiştir.

Anahtar Kelimeler: *Alüminyum, Bor Karbür, Kompozit, Sertlik, Mikroyapı*

Received: 03/02/2020, Revised: 18/05/2020, Accepted: 20/05/2020

I. INTRODUCTION

Metal matrix composites (MMCs) can be reinforced with a ceramic or a carbon-based material into a metal matrix material to improve its strength, corrosion resistance, and wear resistance [1-3]. The most preferred matrix materials are magnesium (Mg), aluminum (Al), and its alloys. Among matrix materials, aluminum is the most commonly used metal for their good elasticity modulus (~68 GPa), excellent machinability, low density (~2.7 g/cm^3), excellent corrosion resistance, and high toughness, especially in automotive and aerospace applications such as construction and engine blocks [4-6]. Also, metal oxides (Al_2O_3, ZrO_2, SiO_2, etc.), metal nitrides (TiN, Si_3N_4, TaN, ZrN, etc.), metal carbides (B_4C, SiC, WC, etc.), and carbon-based materials (graphene nanoplatelets (GNPs), fullerenes, carbon nanotube (CNT)) can be used as the reinforcement material [7]. Among ceramic materials, boron carbide (B_4C) has high Young's modulus (~441x10^3 MPa), high hardness (~3800 HV), high melting point (~2400 °C), and low density (~2.52 g/cm^3) [8, 9]. The use of pure boron carbide (B_4C) as a structural material restricted because of its brittle structure. Hence, B_4C was preferred as a particle reinforcement material in aluminum matrix composites. B_4C reinforced aluminum composites have been utilized from the fields of cycling industrial, aviation industry, and electronic communication due to the functional damping capacity, excellent thermal conductivity, high strength, low density, and high specific stiffness [10, 11].

In general, the squeeze casting, melting, and powder metallurgy (PM) can be used to produce the MMCs [12]. Among these methods, the PM method is remarkable because of its ability to fabricating large-size and complex machine parts [13-15]. Especially, aluminum-based composites might be produced by the PM method due to the widespread use of aluminum in the industrial areas such as in the automotive, aviation, transportation, and space industries [16, 17].

Many researchers have made successful attempts to investigate the production, mechanical, and microstructural properties of Al-B_4C composites [18-24]. Khademian et al. [18] examined the influences of pouring temperature (700, 850, 950 °C) and stirring times (10, 15, 20 min) on the mechanical properties of A356-3%B_4C using stir casting method. The optimum pouring temperature and stirring time were determined as 850 °C and 15 min, respectively. Pang et al. [19] studied the tensile properties of Al6061 alloy and Al6061-12%B_4C-2.5%Al_2O_3 composites. According to test results, the tensile and yield strength determined an increase of ~113% and ~246% when compared to those of the Al6061 alloy. Ipekoglu et al. [20] researched the effect of the reinforcement rates of B_4C (0, 3, 5, 10wt%) and squeeze pressure (P=0, 75, 150 MPa) on the mechanical strength of Al-B_4C composites using the squeeze casting method. The highest mechanical properties (yield stress, hardness, and tensile stress) were detected at the amount of 5wt%B_4C and the squeeze pressure of 150 MPa. To the best of our knowledge, no study is available to investigate the microstructural and mechanical properties of B_4C reinforced aluminum composites with different particle sizes and contents of B_4C fabricated by the powder metallurgy method.

The purpose of this study was to fabricate pure Al and B_4C reinforced aluminum composites with different content (B_4C: 1, 3, 6, 9, 12, 15, 30wt%;) and particle size (B_4C: 3.5 and 20 μm) by the powder metallurgy method. The present study aimed to examine the influences of reinforcement rate and particle size of B_4C on the microstructure, porosity, hardness, apparent density, and compressive strength of Al-B_4C composites.

II. MATERIALS AND METHOD

A. MATERIALS

In the present study, B_4C powders (the theoretical density of 2.52 g/cm^3, the mean particle sizes of ~3.5 μm and ~20 μm, and the purity of 99%) were used as the reinforcement material while atomized pure aluminum powders (the theoretical density of 2.7 g/cm^3, the particle diameter of ~10 μm, the purity of 99%) were used as the matrix material. Aluminum and B_4C powders were provided by Alfa Aesar Inc. (United Kingdom), respectively.

B. METHOD

Figure 1 shows the fabrication scheme of boron carbide reinforced aluminum-based composites by powder metallurgy method. Al powders were mixed in ethanol using the mechanical mixer. At the same time, boron carbide powders (1, 3, 6, 9, 12, 15, 30 wt.%) were ultrasonicated in ethanol by using an ultrasonic dispenser. Then, the boron carbide solution was added to the aluminum solution. The solution was filtered and dried at 45 °C for 12 h. The powders were compacted in stainless steel die under a pressure of 650 MPa. Then, the samples were sintered in a tube furnace for the sintering time (t_S=180 min) and the sintering temperature (T_S=630 °C) under vacuum.

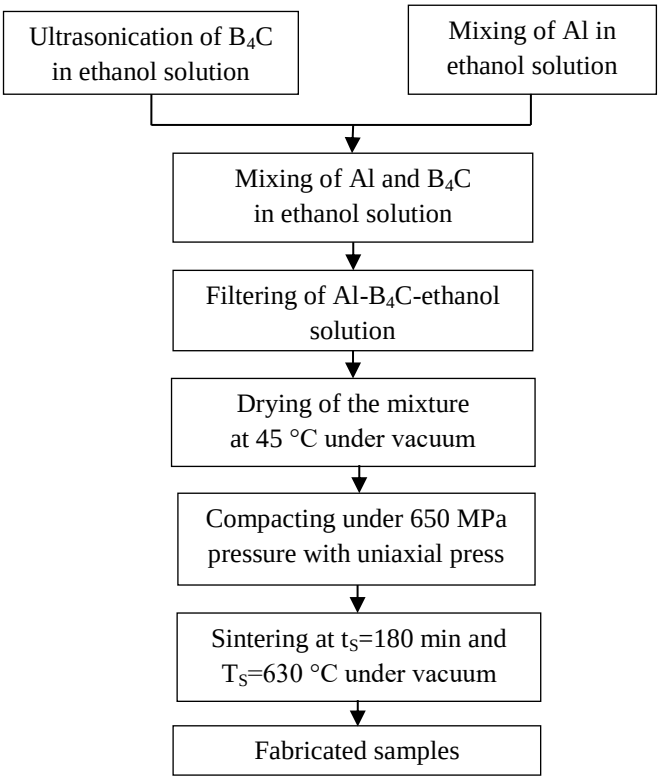

Figure 1. *The fabrication scheme of Al-B_4C composites by the PM method [25]*

The microstructure of composites and powders was determined by using a scanning electron microscope (SEM, Jeol JSM-7001F). SEM analyses were actualized to determine the distribution of boron carbide in the Al matrix. X-ray Diffraction (XRD, Rigaku Smartlab) analysis was used to examine the phases in composites and powders between 20 and 80°. In XRD analysis, raw data were

analyzed afterward, refined by MDI Jade 6.0 program. The apparent densities of the composites were determined by Archimedes' method. The density results were averaged over at least six measurements. The apparent density (ρ_D) can be stated by Eq. (1) [26]:

$$\rho_D = [m_K/(m_D - m_A)]\rho_W \quad (1)$$

where ρ_W is the water density, m_D is the mass of water-saturated composite, m_K is the mass of fabricated composite, and m_A is the mass of the composite submerged in the water.

The theoretical density of the composites (ρ_T) can be determined by Eq. (2):

$$\rho_T = (m_{Al}\% \times \rho_{Al}) + (m_{B4C}\% \times \rho_{B4C}) \quad (2)$$

where m_{B4C}% and m_{Al}% are defined as the mass fraction of B_4C and pure Al, respectively. Also, ρ_{B4C} (2.52 g/cm^3) and ρ_{Al} (2.7 g/cm^3) are defined as the theoretical density of B_4C and pure aluminum, respectively.

The percentage of porosity for the Al-B_4C composites can be calculated by Eq. (3):

$$P\% = (1 - \rho_D/\rho_T) \times 100 \quad (3)$$

The hardness of composites was determined by using a micro Vickers hardness tester under a dwell time of 15 s and a load of 200 g. The measurement was actualized six times from random locations of the polished cross-sections, and then they were averaged. The compressive strength of the composites was detected by the compressive test unit (Mares Test-10 tons). By using this test unit, each sample was tested at least five times with the compression rate of 10 mm/min.

III. RESULTS AND DISCUSSION

A. CHARACTERIZATION OF POWDERS

Scanning electron microscopy images of pure aluminum and boron carbide powders are presented in Figure 2. As seen from the figure, Al powders have nearly spherical morphology. On the other hand, B_4C powders have an irregular form with sharp edges (Figures 2(a-c)). The mean particle size of aluminum is detected as ~10 μm. Also, the mean of boron carbide powders is determined as ~20 μm and ~3.5 μm, respectively (Figures 2(b) and (c)).

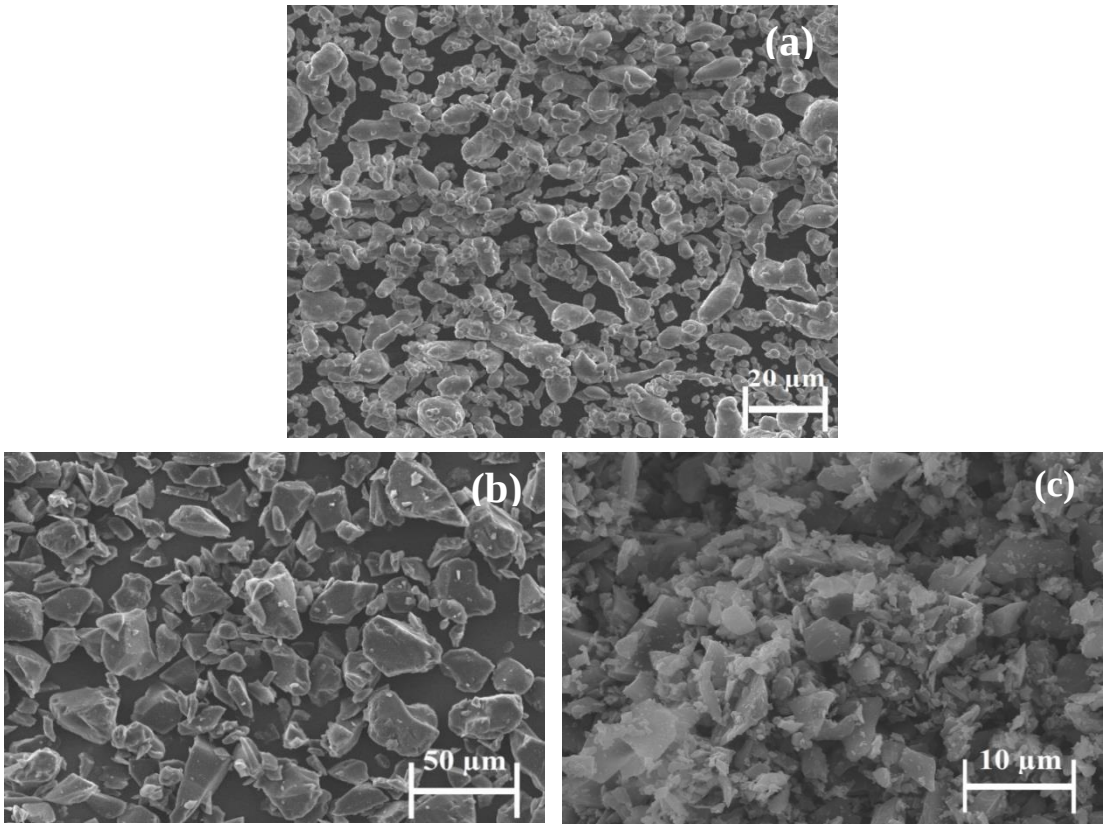

Figure 2. *SEM images of pure Al (a) and B_4C particles (particle sizes of B_4C: 20 µm (b) and 3.5 µm (c))*

XRD plots of pure Al and B_4C were given in Figures 3(a-b), respectively. As shown in these figures, aluminum and B_4C peaks are presented at 2θ=~39°, 45°, 65°, 78 and 2θ=~22°, 23°, 26°, 32°, 35°, 38°, 39°, 50°, 54°, 62°, 64°, 65°, 67°, 70°, 72°, 74°, 75°, 78°, respectively. The phase analyses of pure Al and B_4C particles are an important process to determine the phases of composites after sintering. Also, these analyses give information related to the reaction between the reinforcement and matrix materials after sintering.

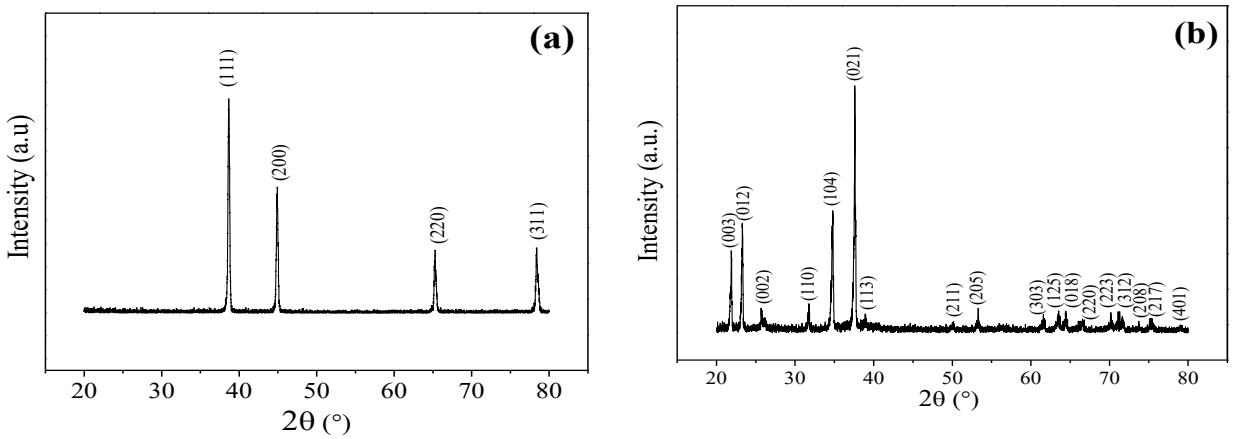

Figure 3. *XRD analyses pure Al (a) and B_4C (b) particles*

B. MECHANICAL PROPERTIES OF COMPOSITES

Figure 4 gives the variation of apparent density and porosity for pure Al and Al-B_4C composites, respectively. As illustrated in Figure 4(a), increasing B_4C content in the aluminum matrix improved the apparent density of Al-B_4C composites. Besides, the decrease in the particle size of the reinforcement material increased the apparent density and decreased the porosity of Al-B_4C composite (Figure 4(b)). The highest density and lowest porosity of the Al-B_4C composite were determined as 2.61 g/cm^3 and 1.4% at Al-B_4C composite with the B_4C particle size of 3.5 µm, respectively. There is an inverse relationship between the porosity and the mechanical properties of the composite. In other words, minimum porosity implies maximum mechanical properties. The density of the Al-B_4C composites improved due to the homogeny dispersion of B_4C in the matrix. It causes the increase of the contact area between the matrix and reinforcement element, which led to the lower porosity and higher density [27, 28].

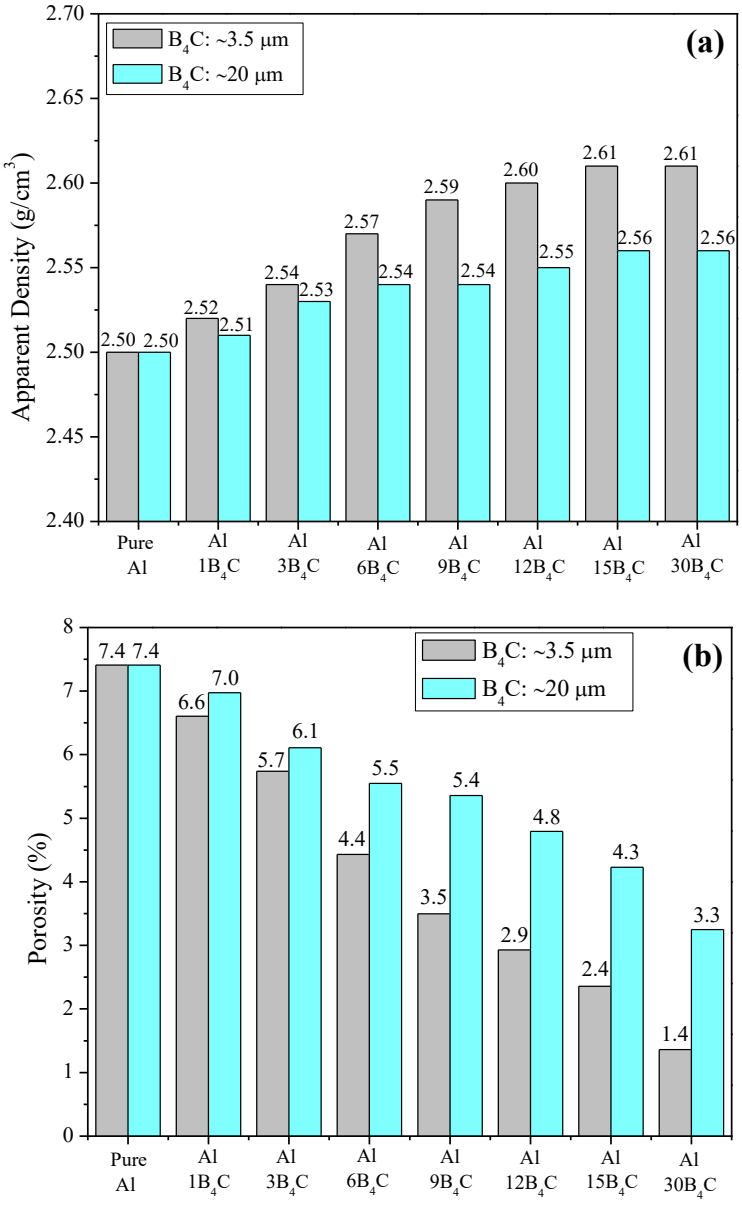

***Figure 4**. Apparent density (a) and porosity (b) variation of pure Al and Al-B_4C composites for different sizes of B_4C particles*

Figure 5 gives the Vickers hardness variation of pure Al and Al-B_4C composites for different sizes of B_4C particles. As shown in the figure, the Vickers hardness of Al-B_4C composites improves with the increase in B_4C amount due to the hard structure of B_4C particles. The highest Vickers hardness (68.8 HV) was obtained at Al-30%B_4C composite. The improvement in Vickers hardness is determined as ~129.3% compare with pure aluminum. Also, an increase in the particle size of B_4C decreases the Vickers hardness of Al-B_4C composites. The increase in the hardness of the composites can be expressed theoretically with the rule of mixtures by Eq. (4) [29].

$$H_c = H_m f_m + H_r f_r \tag{4}$$

where f_m and f_r are the volume fraction of matrix and reinforcement element, H_m, H_c, and H_r are the hardness of the matrix, composite, and reinforcement element, respectively.

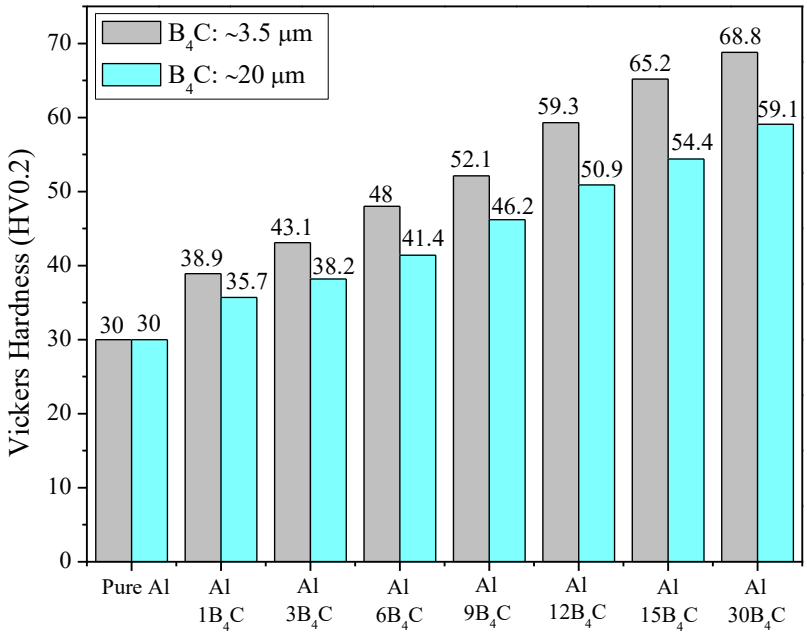

Figure 5. Vickers hardness variation of pure Al and Al-B_4C composites for different sizes of B_4C particles

The compressive strength variation of Al-B_4C and pure Al particles is illustrated in Figure 6. As given in the figure, compressive strength was increased from 91 MPa (pure Al) to 242 MPa (Al-30B_4C). Also, the decrease in the particle size of B_4C from 20 µm to 3.5 µm improves the compressive strength of the fabricated composites from 178 MPa to 242 MPa. In the Al-B_4C composite structure, small B_4C particles act as an obstacle at the aluminum grain boundaries. It prevents the dislocation movement. The decrease between particles by the addition of B_4C particles to the Al matrix declined, and then the dislocation movement blocked. Hence, the mechanical strength of Al-B_4C composites improved. The increase in the strength of the composite can be stated as given in Eq. (5) [29]:

$$\sigma_c = \sigma_m f_m + \sigma_r f_r \tag{5}$$

where f_m, f_r, and f_c are the volume fraction of matrix, reinforcement, and composite material, σ_m, σ_r, and σ_c are the strength of the matrix, reinforcement, and composite material, respectively.

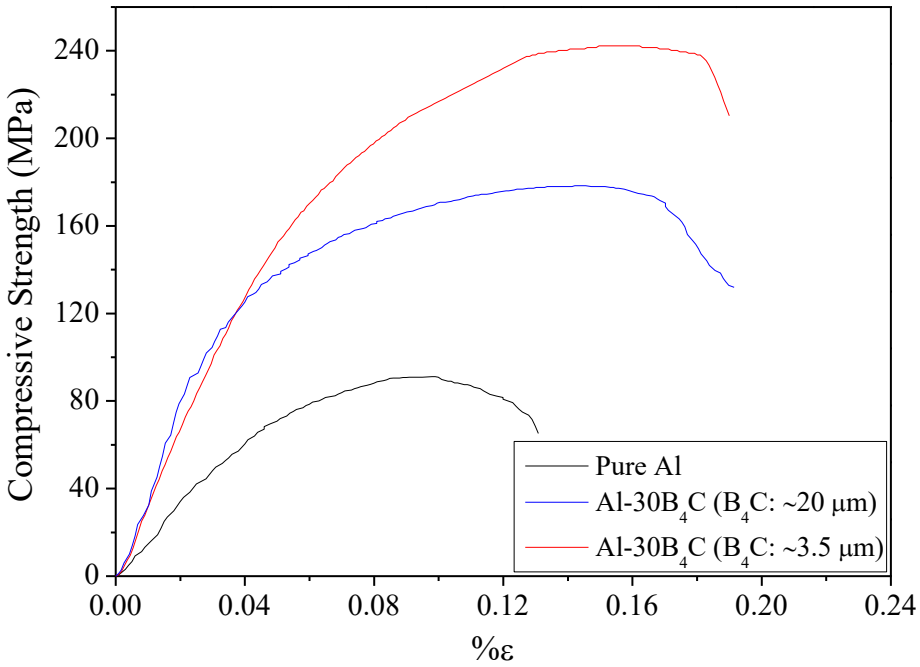

***Figure 6**. Compressive strength variation of pure Al and Al-B_4C composites for different sizes of B_4C particles*

C. CHARACTERIZATION OF SINTERED COMPOSITES

XRD patterns of Al-B_4C composites and pure Al are presented in Figure 7. In order to determine the phase formation in Al matrix composites, XRD analysis was detected for pure Al, Al-15B_4C, and Al-30B_4C. As indicated in the figure, the intensity of B_4C peaks in Al composites increased with increasing B_4C content. The peak angles (2θ=~22°, 23°, 26°, 32°, 35°, 38°, 39°, 50°, 54°, 62°, 64°, 65°, 67°, 70°, 72°, 74°, 75°, 78) of B_4C were confirmed by the existence of B_4C in Al-B_4C composites. According to the XRD analysis, the undesired phase formation, such as Al_4C_3 phases were not observed in any composition.

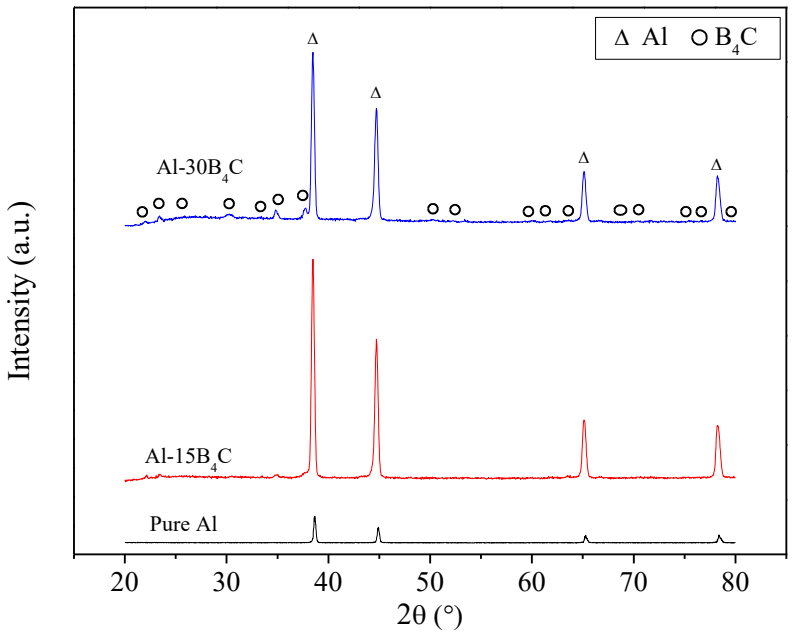

***Figure 7**. XRD plots of pure Al, Al-15B_4C, and Al-30B_4C composites*

Scanning electron microscope (SEM) images of pure aluminum, Al-6B_4C, Al-15B_4C, and Al-30B_4C composites for different sizes of B_4C particles (B_4C: 20 μm and 3.5 μm) are shown in Figures 8 and 9, respectively. As illustrated in Figure 8, it was clearly seen that B_4C particles were distributed homogeneously and positioned at between aluminum boundaries. On the other hand, many pores were detected in the microstructure of the Al-B_4C composite due to bigger particle sizes of B_4C (Figure 8(b-d)). Figure 9 gives the SEM images of pure Al, Al-6B_4C, Al-15B_4C, and Al-30B_4C with a smaller particle sizes of B_4C (3.5 μm), respectively. The homogeny distribution of B_4C particles was detected from the SEM images of Al-B_4C composites. Also, less porosity was observed due to the smaller size of B_4C particles (Figure 9(b-d)). As a result, the mechanical properties (compressive strength and Vickers hardness) of B_4C reinforced aluminum composites with smaller B_4C particle size were better than the mechanical strength of B_4C reinforced aluminum composites with larger B_4C particle size.

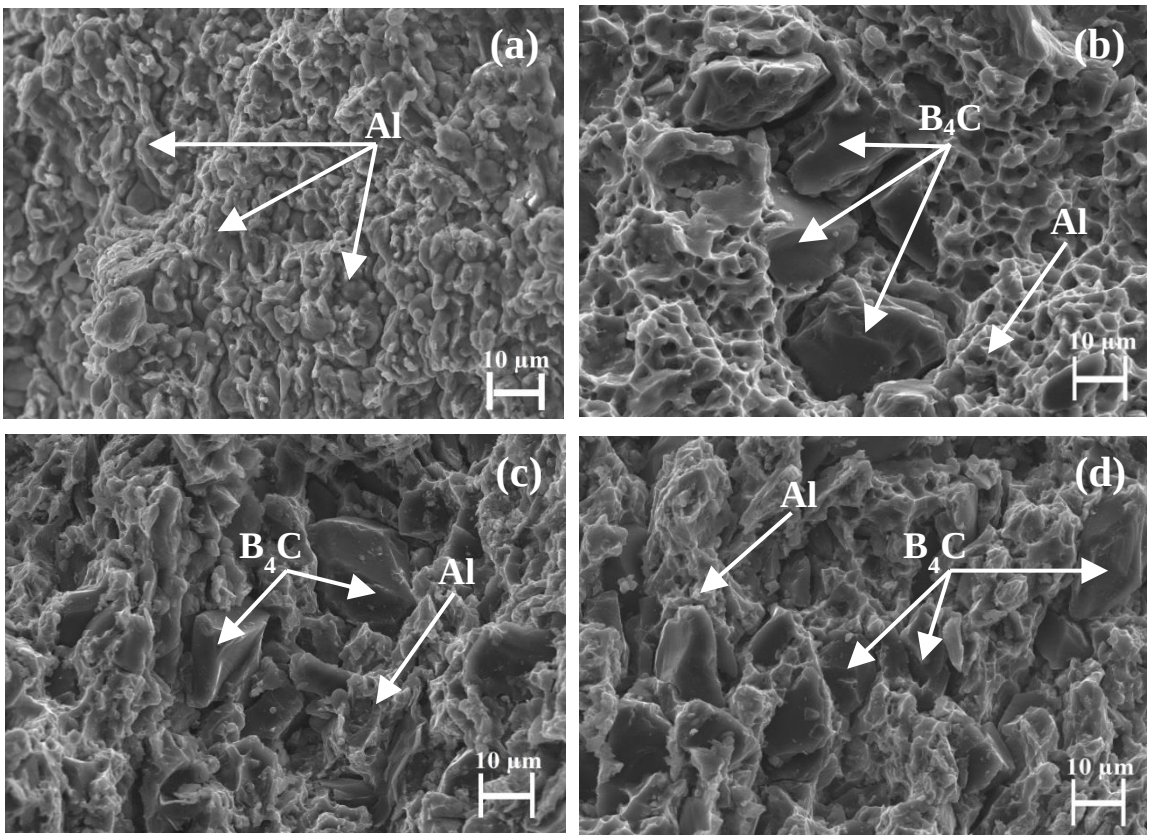

Figure 8. *SEM images of pure Al (a), Al-6B_4C (b), Al-15B_4C (c), and Al-30B_4C (d) composites (particles size of B_4C: 20 μm)*

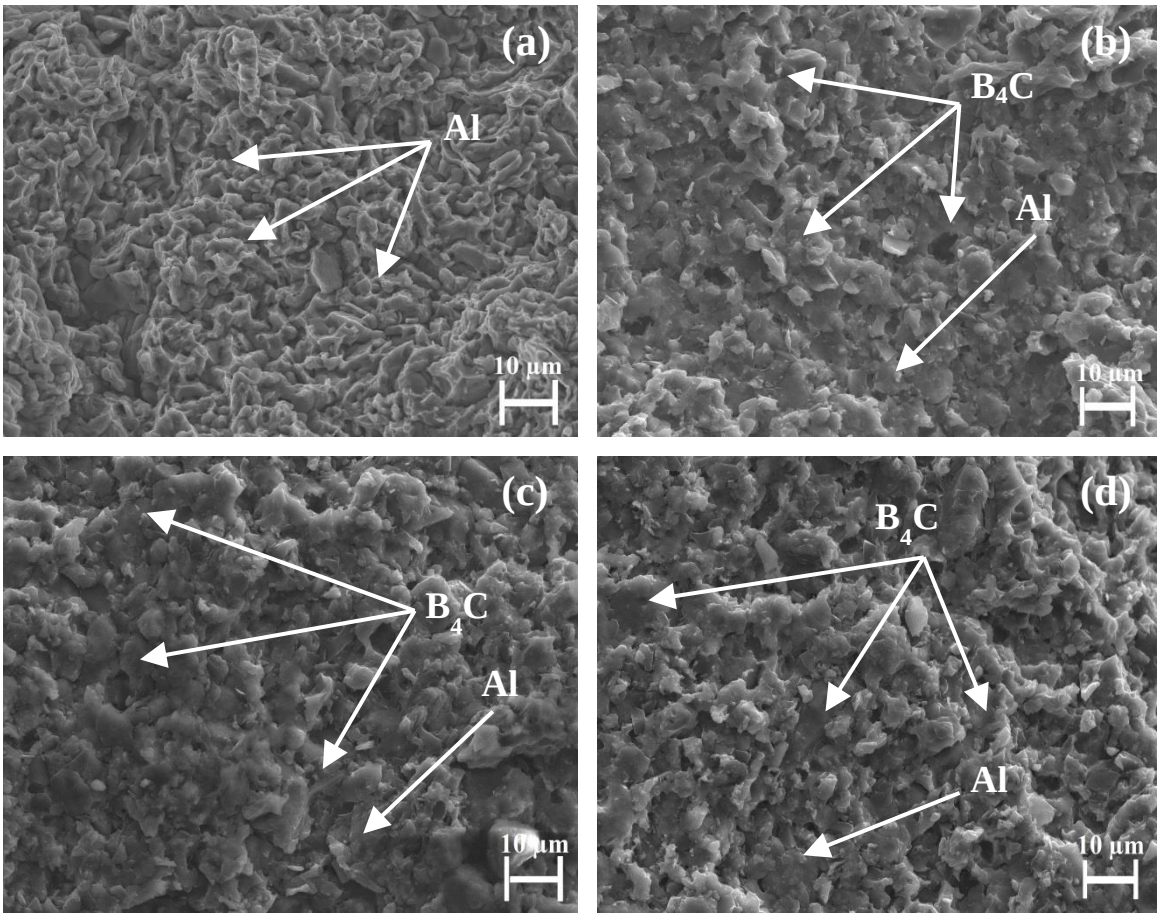

Figure 9. *SEM images of pure Al (a), Al-6B_4C (b), Al-15B_4C (c), and Al-30B_4C (d) composites (particles size of B_4C: 3.5 µm)*

IV. CONCLUSIONS

In the present study, B_4C reinforced aluminum matrix composites with various contents (1, 3, 6, 9, 12, 15, 30wt.%) and particle size (3.5 and 20 µm) of B_4C were fabricated by the powder metallurgy method. The effect of the particle sizes and reinforcement rates of B_4C on the Vickers hardness, the apparent density, porosity, compressive strength, and microstructure of Al-B_4C composites were investigated. According to the test results, the highest apparent density (2.61 g/cm^3), Vickers hardness (68.8 HV), compressive strength (242 MPa), and minimum porosity (1.4%) were obtained at Al-30%B_4C composite with 3.5 µm particle size of B_4C. Well-distributed small B_4C particles act as an obstacle at the grain boundaries. Also, these particles prevent the grain growth during sintering. Hence, reinforcement of small B_4C particles enhances the mechanical strength of Al-based composites owing to the hard structure and high compressive strength of B_4C particles.

V. REFERENCES

[1] G.S. Hanumanth and G.A. Irons, "Particle incorporation by melt stirring for the production of metal-matrix composites," *Journal of Materials Science*, vol. 28, pp. 2459-2465, 1993.

[2] Y. Sahin and S. Murphy, “The effect of fibre orientation on the dry sliding wear of borsic-reinforced 2014 Al alloy,” *Journal of Materials Science*, vol. 34, pp. 5399–5407, 1996.

[3] M. Kok, “Production and mechanical properties of Al_2O_3 particle-reinforced 2024 aluminium alloy composites,” *Journal of Materials Processing Technology*, vol. 161, pp. 381–387, 2005.

[4] K.K. Chawla, *Composite Materials*. New York: Springer, 2006.

[5] D.K. Koli, G. Agnihotri, and R. Purohit, “Advanced aluminium matrix composites: the critical need of automotive and aerospace engineering fields,” *Materials Today: Proceedings*, vol. 2, pp. 3032-3041, 2015.

[6] A. Macke, B.F. Schultz, P., and Rohatgi, “Metal matrix composites offer the automotive industry an opportunity to reduce vehicle weight, improve performance,” *Advanced Materials&Proceedings*, vol. 170, pp. 19-23, 2012.

[7] J.K. Chen and I.S. Huang, “Thermal properties of aluminum–graphite composites by powder metallurgy,” *Composites Part B-Engineering*, vol. 44, no. 1, pp. 698–703, 2013.

[8] T.M. Lillo, “Enhancing ductility of Al6061+10 wt.% B_4C through equal-channel angular extrusion processing,” *Materials Science and Engineering A-Structural Materials*, vol. 410-411, pp. 443-446, 2005.

[9] A. Alizadeh, E. Taheri-Nassaj and H.R. Baharvandi, B. “Preparation and investigation of Al-4wt%B_4C nanocomposite powders using mechanical milling,” *Bulletin of Materials Science*, vol. 34, no. 5, 1039-1048, 2011.

[10] H.M. Hu, E.J. Lavernia, W.C. Harrigan, J. Kajuch and S.R. Nutt, “Microstructural investigation on B_4C/Al-7093 composite,” *Materials Science and Engineering A-Structural Materials*, vol. 297, no. 1-2, pp. 94-104, 2001.

[11] V.M. Ravindranath, G.S. Shiva Shankar, S. Basavarajappa, and N.G. Siddesh Kumar, “Dry sliding wear behavior of hybrid aluminum metal matrix composite reinforced with boron carbide and graphite particles,” *Materials Today: Proceedings*, vol. 4, no. 10, pp. 11163-11167, 2017.

[12] A. Saboori, C. Novara, M. Pavese, C. Padini, F. Giorgis, P. Fino, “An investigation on the sinterability and the compaction behavior of aluminum/graphene nanoplatelets (GNPs) prepared by powder metallurgy,” *Journal of Materials Engineering and Performa*nce, vol. 26, no. 3, pp. 993-999, 2017.

[13] G. O’Donnel and L. Looney, “Production of aluminium matrix composite components using conventional PM technology,” *Materials Science and Engineering A-Structural Materials*, vol. 303, issue. 1-2, pp. 292–301, 2001.

[14] O.G. Neikow, S.S. Naboychenko, and G. Dawson, *Handbook of non-ferrous metal powders-technologies and applications*. Amsterdam: Elsevier, 2009.

[15] R.S. Rana, R. Purohit, V.K. Soni, S. Das, "Characterization of mechanical properties and microstructure of aluminium alloy-SiC composites," *Materials Today: Proceedings*, vol. 2, no. 4-5, pp. 1149-1156, 2015.

[16] M. Zamani, H. Dini, A. Svoboda, L. Lindgren, S. Seifeddine, N. Andersson, A.E.W. Jarfors, "A dislocation density based constitutive model for as-cast Al-Si alloys: effect of temperature and microstructure," *International Journal of Mechanical Sciences*, vol. 121, pp. 164–170, 2017.

[17] N. Srivastava and G.P. Chaudhari, "Microstructural evolution and mechanical behavior of ultrasonically synthesized Al6061-nano alumina composites," *Materials Science and Engineering A-Structural Materials*, vol. 724, pp. 199-207, 2018.

[18] M. Khademian, A. Alizadeh A. Abdollahi, "Fabrication and characterization of hot rolled and hot extruded boron carbide (B_4C) reinforced A356 aluminum alloy matrix composites produced by stir casting method," *Transactions of the Indian Institute of Metals*, vol. 70, no. 6, pp. 1635-1646, 2017.

[19] X. Pang, Y. Xian, W. Wang, P. Zhang, "Tensile properties and strengthening effects of 6061 Al/12wt%B_4C composite reinforced with nano-Al_2O_3 particles," Journal of Alloys and Compounds, vol. 768, pp. 476-484, 2018.

[20] M. Ipekoglu, A. Nekouyan, O. Albayrak, S. Altintas, "Mechanical characterization of B_4C reinforced aluminum matrix composites produced by squeeze casting," *Journal of Materials Research*, vol. 32, pp. 599-605, 2017.

[21] S. Dhandapani, T. Rajmohan, K. Palanikumar, M. Charan, "Synthesis and characterization of dual particle (MWCNT+B_4C) reinforced sintered hybrid aluminum matrix composites," *Particulate Science and Technology*, vol. 34, pp. 255-262, 2016.

[22] S. Das, M. Chandrasekaran, S. Samanta, "Comparison of mechanical properties of AA6061 reinforced with (SiC/B_4C) micro/nano ceramic particle reinforcements," *Materials Today: Proceedings*, vol. 5, no.9, pp. 18110-18119, 2018.

[23] B. Ravi, B.B. Naik, J.U. Prakash, "Characterization of aluminum matrix composites (AA6061/B_4C) fabricated by stir casting technique," *Materials Today: Proceedings*, vol. 2, no.4-5, pp. 2984-2990, 2018.

[24] G.S. Saini and S. Goyal, "Fabrication and microstructure study of aluminum matrix composites reinforced with SiC and B_4C particulates," *Nano Hybrid and Composites*, vol. 16, pp. 26-29, 2017.

[25] M.C. Şenel, M. Gürbüz, E. Koç, "The fabrication and characterization of synergistic Al-SiC-GNPs hybrid composites," *Composites Part B-Engineering*, vol. 154, pp. 1-9, 2018.

[26] M. Gürbüz, M.C. Şenel, E. Koç, "The effect of sintering temperature, time and graphene addition on the mechanical properties and microstructure of aluminum composites," *Journal of Composite Materials*, vol. 52, no. 4, pp. 553-563, 2018.

[27] T. Varol and A. Canakci, "Microstructure, electrical conductivity and hardness of multilayer graphene/copper nanocomposites synthesized by flake powder metallurgy," *Metals and Materials International*, vol. 21, no. 4, pp. 704-712, 2015.

[28] M. Rahimian, N. Ehsani, N. Parvin, H.R. Baharvandi, “The effect of particle size, sintering temperature and sintering time on the properties of $Al–Al_2O_3$ composites, made by powder metallurgy,” *Journal of Materials Processing Technology*, vol. 209, no. 14, pp. 5387-5393, 2009.

[29] G.E. Dieter, *Mechanical Metallurgy*. New York: McGraw-Hill, 1986.